Breakdown of superfluidity of an atom laser past an obstacle

Nicolas Pavloff*

Laboratoire de Physique Théorique et Modèles Statistiques, Université Paris Sud, Bâtiment 100, F-91405 Orsay Cedex, France
(Received 27 March 2002; published 19 July 2002)

The one-dimensional flow of a continuous beam of Bose-Einstein condensed atoms in the presence of an obstacle is studied as a function of the beam velocity and of the type of perturbing potential (representing the interaction of the obstacle with the atoms of the beam). We identify the relevant regimes: stationary/time-dependent and superfluid/dissipative; the absence of drag is used as a criterion for superfluidity. There exists a critical velocity below which the flow is superfluid. For attractive obstacles, we show that this critical velocity can reach the value predicted by Landau's approach. Besides, for penetrable obstacles, it is shown that superfluidity is recovered at large beam velocity. Finally, enormous differences in drag occur when switching from repulsive to attractive potential.

I. INTRODUCTION

The rapid progresses in the technology of guiding cold atoms (using hollow optical fibers [1], magnetic guides [2], and microchips [3]) opens up the prospect of similar studies of guided Bose-Einstein condensed beams, i.e., of guided continuous atom lasers. Indeed, important progress in this direction is presently being made, which uses the techniques developed for guiding cold atoms: waveguides have been designed for a Bose-Einstein condensate using a blue-detuned hollow laser beam [4]; Bose condensation has been obtained over a microchip [5,6] and a Bose-Einstein wave packet has been propagated in a microfabricated magnetic waveguide [7]. Also, a continuous beam of cold atoms has been loaded into a magnetic guide, as a first step in order to perform evaporative cooling and condensation in the guide [8].

In the present work, we address the question of superfluidity of a continuous (guided) atom laser, namely, what are the conditions for the flow to be dissipationless? A criterion for superfluidity has been proposed long ago by Landau [9] which states that dissipation does not occur if the velocity of the flow is lower than the critical value $v_{\rm crit} = \min\{E(q)/q\}$, where $E(q)$ is the energy of an excitation with momentum q.

Many experiments have been done in liquid helium II to test Landau's idea, and indeed one finds a critical velocity, but in many instances it is much lower than Landau's expectation. As Feynman first suggested [10], this is linked to vortex formation, i.e., to nonlinear perturbation of the fluid (and not to elementary excitations as implied by Landau [11]). The experiments done at MIT for Bose-Einstein condensates confirm this view: in these systems, there is also a critical velocity [12,13], it is lower that Landau's expectation, and it is also linked to vortex formation [14].

In the following, we are concerned with one-dimensional flows, which are relevant to atom laser physics. We devise an alternative phrasing of Landau's argument based on perturbation theory and identify its limit of validity. In the generic, nonperturbative case, we confirm that, for obstacles represented by *repulsive potentials*, dissipation begins at a velocity lower than the one expected on the basis of Landau's argument and corresponds to emission of solitons (which are the one-dimensional analogues of vortices). However, we show that Landau's critical velocity is always reached for *attractive potentials*. Furthermore, following a previous study [15], above Landau's critical velocity we identify a new (numerically stable) regime, stationary *and* dissipative. In this regime, the drag exerted on an obstacle can be computed with little numerical effort. Moreover, in this regime, we show that at large velocity the drag exerted on a penetrable obstacle goes to zero, i.e., superfluidity is recovered.

The paper is organized as follows. In Sec. II, we set up the theoretical framework and notations. The natural criterion for the breakdown of superfluidity is the absence of drag, and in this section we show precisely how the drag can be computed. In Sec. III, we determine the different types of flow and the corresponding drag for an obstacle represented by an external potential (a weak potential in Sec. III A, a δ peak in Sec. III B, a square well in Sec. III C, and a Gaussian potential in Sec. III D). Finally, we discuss our results in Sec. IV, where we emphasize the important differences between attractive and repulsive potentials in the nonlinear regime.

II. A CRITERION FOR SUPERFLUIDITY

We work in a quasi-one-dimensional regime, or more precisely, we use an adiabatic approximation where the condensate wave function $\Psi(\vec{r},t)$ can be cast in the form [16,15]

$$\Psi(\vec{r},t) = \psi(x,t)\phi(\vec{r}_\perp;n), \qquad (1)$$

where $\psi(x,t)$ describes the motion along the axis of the laser. ϕ is the equilibrium wave function (normalized to unity) in the transverse ($\vec{r}_\perp$) direction; it depends parametrically on the longitudinal density $n(x,t) = \int d^2r_\perp |\Psi|^2 = |\psi(x,t)|^2$. The beam is confined in the transverse direction by a trapping potential $V_\perp(\vec{r}_\perp)$. The adiabatic approximation assumes that the transverse scale of variation of the profile is much smaller than the longitudinal one. The transverse degrees of freedom are not completely frozen, but adapt to the smooth longitudinal dynamics: this is the essence of the parametric dependence of ϕ on $n(x,t)$. This represents a significant im-

*Email address: pavloff@ipno.in2p3.fr

provement to what is generally defined as a quasi-one-dimensional approach and results in a nontypical nonlinearity of the one dimensional (1D) reduction of the Gross-Pitaevskii equation below [Eqs. (2) and (3)].

In the regime in which Eq. (1) holds [17], the equation governing the time evolution of $\psi(x,t)$ reads [16,15] (we set units such that $\hbar = m = 1$)

$$-\tfrac{1}{2}\partial_{xx}^2\psi + \{V_{\parallel}(x) + \epsilon[n(x,t)]\}\psi = i\partial_t\psi. \qquad (2)$$

In Eq. (2), $V_{\parallel}(x)$ represents the effect of the obstacle. We restrict ourselves to the case of a localized perturbation with $\lim_{x\to\pm\infty}V(x)=0$. Such an obstacle can be realized by crossing the trajectory of the atom laser with a detuned optical laser beam whose waist is large compared with the perpendicular extension of the condensed beam. Another possibility is to bend the trajectory of the guided atom laser; this results in an attractive effective potential proportional to the square of the curvature (see [15]).

$\epsilon(n)$ is a nonlinear term describing the mean-field interaction inside the beam, and the way it is affected by the transverse confinement. For a transverse confining harmonic potential of pulsation $\omega_{\perp}$, one has (see [15])

$$\epsilon(n) = 2\omega_{\perp}na_{sc} \text{ in the low-density regime, } na_{sc}\ll 1,$$

$$\epsilon(n) = 2\omega_{\perp}\sqrt{na_{sc}} \text{ in the high-density regime, } na_{sc}\gg 1, \qquad (3)$$

where a_{sc} denotes the s-wave scattering length of the two-body interatomic potential (we consider only the case $a_{sc} > 0$, i.e., a repulsive effective interaction). In the following, we use a formalism allowing to treat both the high- and the low-density regime, since both will be of interest in future guided-atom laser experiments.

We want to characterize the superfluidity of the flow past the obstacle. To this end, we compute the drag F_d exerted by the atom laser on the obstacle: a finite drag implies dissipation, whereas $F_d = 0$ corresponds to a superfluid flow. F_d is defined as

$$F_d(t) = \int_{-\infty}^{+\infty} dx\, n(x,t)\frac{dV_{\parallel}(x)}{dx}. \qquad (4)$$

This definition is quite natural: the force exerted on the obstacle is the mean value of the operator $dV_{\parallel}(x)/dx$ over the condensate wave function. It is rigorously justified by the analysis below in term of a stress tensor [Eq. (6)].

For analytical determination of the drag, we use the following procedure: the 1D version of the stress tensor of the fluid is [18]

$$T(x,t) = -\text{Im}(\psi^*\partial_t\psi) + \tfrac{1}{2}|\partial_x\psi|^2$$
$$\qquad - \varepsilon[n(x,t)] - V_{\parallel}(x)n(x,t),$$
$$\text{where } \varepsilon(n) = \int_0^n \epsilon(\rho)d\rho, \qquad (5)$$

and its impulsion density is $J(x,t) = \text{Im}(\psi^*\partial_x\psi)$ (in our units, it is also the current density). By the conservation equation $\partial_t J + \partial_x T + n\,\partial_x V_{\parallel} = 0$, the total impulsion of the beam $P(t) = \int_{-\infty}^{+\infty}dx\,J(x,t)$ is related to F_d by

$$\frac{dP}{dt} = T(-\infty,t) - T(+\infty,t) - F_d(t). \qquad (6)$$

The physical content of Eq. (6) is clear: dP/dt equals the total force exerted over the beam. One part of this force $(-F_d)$ is due to the potential, the other one is the stress on the boundaries of the beam (at left and right infinity). Hence Eq. (6) confirms the heuristic guess (4); besides, it allows us to determine the drag in a simple fashion in the stationary regime where T and P are time-independent:

$$F_d = T(-\infty) - T(+\infty) \text{ in the stationary regime.} \qquad (7)$$

Hence, in the following, we devote particular attention to stationary solutions of Eq. (2). They are of the form $\psi(x,t) = \exp\{-i\mu t\}A(x)\exp\{iS(x)\}$, with A and S real functions. The density is $n(x) = A^2(x)$, the velocity $v(x) = dS/dx$, and the current $J(x) = n(x)v(x)$ is a constant that we note J_∞. From Eq. (2), the amplitude $A(x)$ obeys a Schrödinger-like equation,

$$-\frac{1}{2}\frac{d^2A}{dx^2} + \left\{V_{\parallel}(x) + \epsilon[n(x)] + \frac{J_\infty^2}{2n^2(x)}\right\}A(x) = \mu A(x). \qquad (8)$$

As discussed in [15], the radiation condition requires that solutions of Eq. (8) have no wake far downstream: long-range perturbations of the beam only occur upstream. Hence the boundary conditions have to be imposed downstream: because of nonlinearity, one cannot disentangle an incident and a reflected part in the perturbed upstream flow. In the following, we take a beam going in the negative x direction, with downstream boundary conditions $n(x\to-\infty) = n_\infty$ and $v(x\to-\infty) = -v_\infty$ (with $v_\infty > 0$). Then, the chemical potential is $\mu = v_\infty^2/2 + \epsilon(n_\infty)$. In the following, we refer to v_∞ as the beam velocity and to $c_\infty = (n_\infty d\epsilon/dn|_{n_\infty})^{1/2}$ as the sound velocity (the proper denomination should be "sound velocity evaluated at constant density n_∞"). We also express the lengths in units of the relaxation length $\xi = [2\epsilon(n_\infty)]^{-1/2}$.

For stationary flows, the stress tensor (5) reads

$$T(x) = \frac{1}{2}\left(\frac{dA}{dx}\right)^2 + W[n(x)] - V_\parallel(x)n(x),$$

$$\text{where} \quad W(n) = -\varepsilon(n) + \mu n + \frac{J_\infty^2}{2n}. \tag{9}$$

In regions where the spatial variations of $V_\parallel(x)$ are negligible, $T(x)$ is a constant [as easily seen from Eq. (8)].

$$\delta A(x) = \begin{cases} -\dfrac{\sqrt{n_\infty}}{\kappa}\displaystyle\int_{-\infty}^{+\infty} V_\parallel(y)\exp\{-\kappa|x-y|\}dy & \text{when} \quad v_\infty < c_\infty, \\[14pt] \dfrac{2\sqrt{n_\infty}}{\kappa}\displaystyle\int_{-\infty}^{x} V_\parallel(y)\sin\{\kappa(x-y)\}\,dy & \text{when} \quad v_\infty > c_\infty. \end{cases} \tag{10}$$

The asymptotic evaluation of Eq. (10) when $x \to \pm\infty$ allows us to compute the drag through Eq. (7). From Eqs. (9) and (10), $T(-\infty)$ and $T(+\infty)$ differ only in the supersonic case where

$$T(-\infty) = W(n_\infty),$$

$$T(x \to +\infty) = T(-\infty) + \frac{1}{2}\left(\frac{d\,\delta A(x)}{dx}\right)^2 + \frac{\kappa^2}{2}\delta A^2(x), \tag{11}$$

with (always in the supersonic regime)

$$\delta A(x) \underset{x \to +\infty}{\sim} \frac{2\sqrt{n_\infty}}{\kappa}\,\text{Im}\{e^{i\kappa x}\hat{V}_\parallel(\kappa)\}, \tag{12}$$

and $\hat{V}_\parallel(\kappa) = \int_{-\infty}^{+\infty} dx\,\exp(-i\kappa x)V_\parallel(x)$ is the Fourier transform of $V_\parallel(x)$. One thus obtains

$$F_d = 0 \quad \text{when} \quad v_\infty < c_\infty,$$

$$F_d = -2n_\infty|\hat{V}_\parallel(\kappa)|^2 \quad \text{when} \quad v_\infty > c_\infty. \tag{13}$$

The gross behavior characterized by Eq. (13) is general: at low velocity, the flow is superfluid, whereas at high velocity dissipation occurs. This corresponds to Landau's criterion, which determines a critical velocity below which the flow is dissipationless: $v_{\text{crit}} = \min\{E(q)/q\}$, where $E(q)$ is the energy of an excitation with momentum q. For our system, $E(q)$ is given by the Bogoliubov dispersion relation $E(q) = q\,(c_\infty^2 + q^2/4)^{1/2}$ (see, e.g., [19]) and the Landau critical velocity is then $v_{\text{crit}} = c_\infty$. Hence the present perturbative approach is identical to Landau's criterion since both give the same value of velocity for the onset of dissipation and have the same physical content: excitation of small, nonlocalized perturbations is allowed only above v_{crit}.

However, Landau's criterion, as well as the reasoning leading to Eq. (13), are, by essence, perturbative. We show

III. DETERMINATION OF THE DRAG

A. Perturbative solution

Let us first evaluate the drag experienced by the obstacle when the effects of the potential $V_\parallel(x)$ on the flow can be treated perturbatively. In this case, by adiabatically branching the potential, one can always find a stationary solution with $A(x) = \sqrt{n_\infty} + \delta A(x)$ having the correct boundary condition (i.e., verifying the radiation condition). Introducing the notation $\kappa = 2|v_\infty^2 - c_\infty^2|^{1/2}$, one finds (see [15])

below that, as discussed in the Introduction, nonlinear effects alter these simple perturbative views.

B. δ-peak potential

A first hint of the failure of the perturbative approach can be obtained by studying the effect on the flow of a delta potential $V_\parallel(x) = \lambda\,\delta(x)$. In that case, a stationary solution is obtained by matching two free propagation modes of the laser [i.e., solutions of Eq. (8) in the absence of a potential] at $x = 0$ with the condition $A'(0^+) - A'(0^-) = 2\lambda A(0)$. The upstream and downstream stress tensors are constant; they are related by $T_{\text{up}} = T_{\text{down}} + \lambda A(0)[A'(0^-) + A'(0^+)]$. Besides, at velocity $v_\infty > c_\infty$, the radiation condition imposes that the downstream ($x < 0$) density is constant: this gives $n(0) = n_\infty$ and $A'(0^-) = 0$. Hence, for beam velocity v_∞ larger than c_∞, in the stationary regime Eq. (7) yields

$$F_d = -2n_\infty\lambda^2. \tag{14}$$

The same formula would have been obtained by using the perturbative result (13). Hence it may seem that the perturbative approach is valid for all range of δ potentials and velocities. However, one would expect perturbation to fail for strong potentials and near $v_\infty = c_\infty$, since it is meaningful only if $|\delta A(x)| \ll \sqrt{n_\infty}$, i.e., if $|\lambda| \ll \kappa = 2\,|v_\infty^2 - c_\infty^2|^{1/2}$ [see Eq. (10)]. Indeed, whereas a naive perturbative approach [leading to Eq. (10)] predicts that a stationary solution exists for all values of v_∞, an exact solution in the presence of a δ potential can be found only in some precise range of velocity and potentials. This has been studied in Ref. [15] and is illustrated in Fig. 1. Roughly speaking, stationary regimes only exist for low and high values of v_∞ (in the shaded zone of Fig. 1). In the low-velocity case, the stationary profile is a trough (or a bump, depending on the sign of the potential) localized on the perturbation [20]. Such flows are dissipationless. At high velocity, the stationary profile has a (nonlinear) wake extending to infinity in the upstream direction
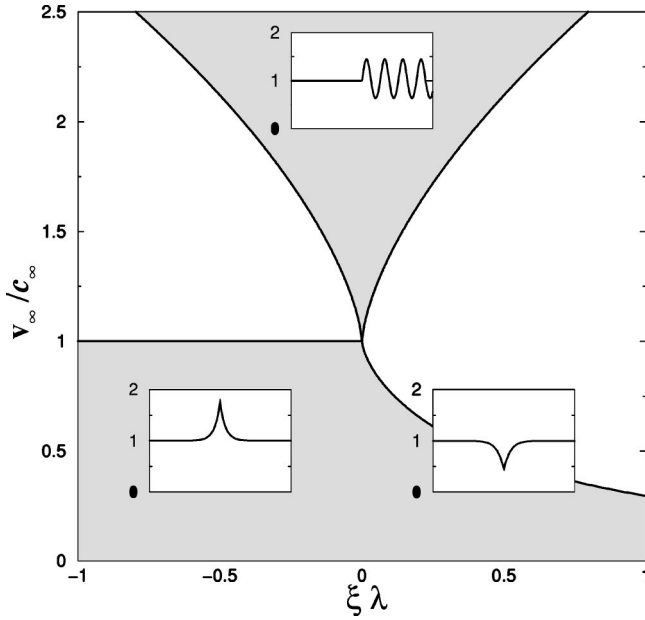
FIG. 1. The shaded zone of the plane (v_∞, λ) is the domain of existence of stationary solutions occurring for a potential $V_\parallel(x) = \lambda \delta(x)$. The axes are labeled in dimensionless units. The insets represent density profiles $n(x)/n_\infty$ typical for the different flows (the condensed beam is incident from the right). Each inset is located at values of v_∞ and λ typical for the flow it displays. The left (right) lower one is a superfluid flow across an attractive (repulsive) potential. The upper one is a dissipative flow.

and this corresponds to dissipation [by Eq. (7)]. In between, the flow is time-dependent and there is no reason why, in this case, the drag should be given by Eq. (14).

We note here an important dissymmetry between repulsive ($\lambda > 0$) and attractive ($\lambda < 0$) potentials: the domain of superfluid flow extends up to $v_\infty = c_\infty$ for $\lambda < 0$, i.e., the critical velocity has the same value as the one predicted by Landau's approach. On the other hand, for $\lambda > 0$ the critical velocity is potential-dependent and decreases significantly. This feature is very general (it occurs for all the other potentials we have studied). We will comment on it more thoroughly in Sec. III D and in the Conclusion.

C. Repulsive square well

Another case with analytical stationary solutions is the repulsive square well: $V_\parallel(x)$ is zero, except for $0 < x < \sigma$, where it takes the constant and positive value V_0. In this case Eq. (4) yields

$$F_d(t) = V_0[n(0,t) - n(\sigma, t)]. \qquad (15)$$

In the stationary subsonic regime, one can show that $n(\sigma) = n(0)$ (see [15]) and the drag is zero: this characterizes a superfluid flow. For $v_\infty > c_\infty$ instead, Eq. (15) yields a finite drag. In this case, when the flow is stationary, $n(0) = n_\infty$ and $n(\sigma)$ in Eq. (15) can be computed by quadrature, as a solution of
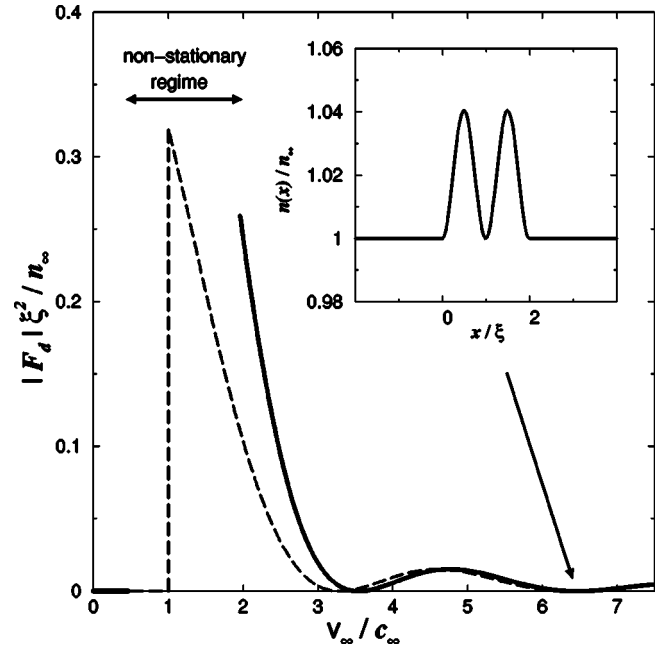

FIG. 2. Drag exerted by a high-density beam on a repulsive square well ($V_0 \xi^2 = 0.2$, $\sigma = 2\xi$), as a function of the beam velocity (F_d and v_∞ are expressed in dimensionless units). The dashed line is the perturbative result (13). The solid line is the exact drag (15). It is evaluated here only in the stationary regime. The inset represents the beam density in the supersonic regime, at a value of velocity (indicated by the arrow) where the drag is exactly zero.

$$\sqrt{2} \left| \sigma - L_0 \text{Int}_n\left(\frac{\sigma}{L_0}\right) \right| = \int_{\sqrt{n_\infty}}^{\sqrt{n(\sigma)}} \frac{dA}{[T_0 - W(n) + V_0 n]^{1/2}}, \qquad (16)$$

where Int_n denotes the nearest integer, L_0 is the period of density oscillations inside the well (which is also expressible as an integral), and $T_0 = W(n_\infty) - V_0 n_\infty$ is the constant value assumed by $T(x)$ inside the well. Of course, Eq. (16) is only valid for a hypersonic stationary solution. In the regime where no stationary solution exists, the drag is time-dependent and should be computed numerically (as done in Sec. III D below).

Figure 2 displays the evolution of the drag as a function of the beam velocity v_∞. The drag has been computed only in the stationary regimes. In the subsonic stationary regime it is exactly zero [20]. In the supersonic stationary regime the exact result (15) (solid line) has been computed in two ways: through the numerical solution of Eq. (16), and also by numerical integration of Eq. (8). Both methods agree within four digits. The exact expression is compared in Fig. 2 with the perturbative result (13) [where the Fourier transform of the potential here gives $|\hat{V}_\parallel(\kappa)|^2 = (2V_0/\kappa)^2 \sin^2(\kappa\sigma/2)$]. For large velocities, the perturbative approach becomes more and more accurate. This is expected from Eq. (10) since, when $\kappa\sigma \gg 1$ (i.e., at large velocities), the perturbative solution is accurate if $V_0 \ll \kappa^2$.

One can remark in Fig.2 that, even in the supersonic regime, the drag happens to be exactly zero for some specific values of v_∞ [21]. As illustrated in the inset, this occurs when
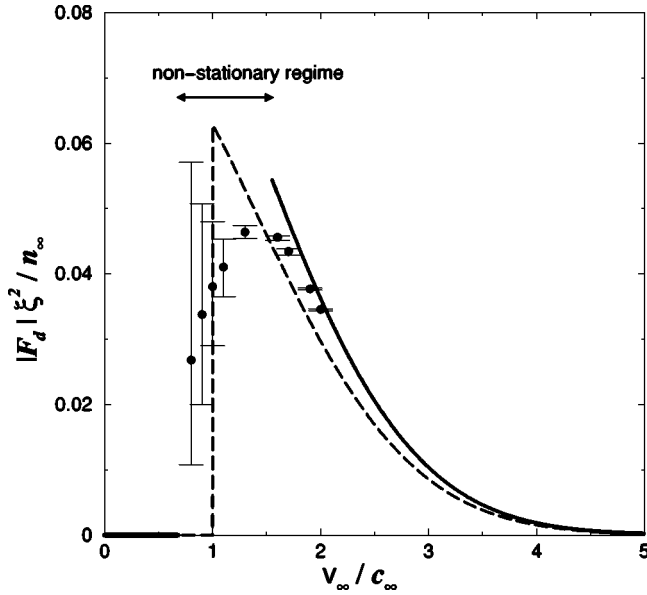
FIG. 3. Drag exerted by a low-density beam on a Gaussian potential $[V_0\xi^2=0.2, \sigma=0.5\xi]$, as a function of the beam velocity. The conventions are the same as in Fig. 2. The dashed line is the perturbative result (13). The solid line is the exact drag evaluated in the stationary regime. The circles correspond to the drag evaluated in the time-dependent regime. The error bars correspond to the extremal values of the time dependent $F_d(t)$ (see the text).
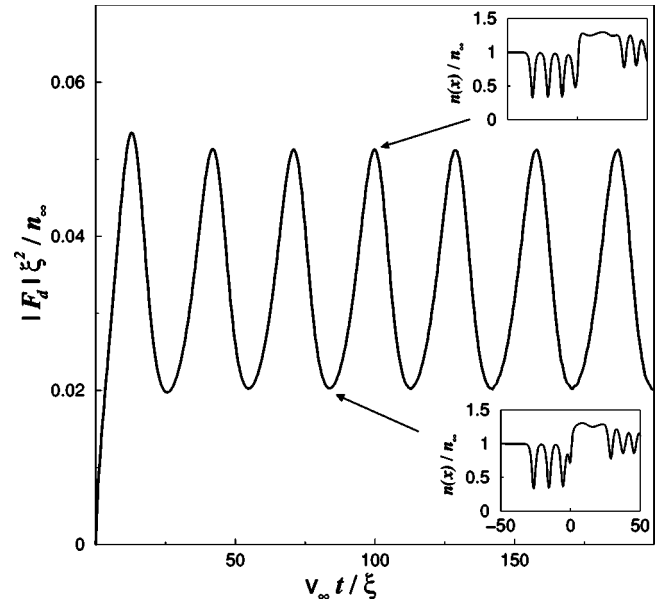

FIG. 4. Time evolution of the drag exerted by a low-density beam (of velocity $v_\infty=0.9c_\infty$) on a Gaussian potential ($V_0\xi^2 =0.2, \sigma=0.5\xi$). F_d and t are expressed in dimensionless units. The upper (lower) inset represents a density profile observed when the drag is maximum (minimum).

the period of the density oscillations inside the well is an exact divisor of its width σ. In this case, the density is unperturbed outside the well. The modification of density inside the well is minute in the case represented in the figure (4%). However, for stronger potentials it can be quite substantial: for $\sigma=2\xi$ and $V_0\xi^2=5$, the maximum density inside the well reaches $2n_\infty$ while the density remains unperturbed (i.e., equal to n_∞) outside the well.

D. Gaussian potential

The generality of the above deductions, based on the study of model potentials (a δ peak and a square well) can be tested numerically on more realistic potentials. We now consider the case $V_\parallel(x)=V_0\exp\{-x^2/\sigma^2\}$ (with $V_0>0$).

As in the previous cases, stationary solutions exist only if the beam velocity v_∞ is not too close to the sound velocity c_∞. In the subsonic stationary regime, the density is perturbed only in the vicinity of the potential, and the flow is superfluid [by Eq. (7)]. In the supersonic stationary regime, the density oscillations extend upstream to infinity, and this corresponds to dissipation. At velocities where a stationary regime is possible, we have determined the drag indifferently using Eq. (4) or Eq. (7) [after having solved Eq. (8) numerically], whereas in the nonstationary case we used Eq. (4) after having solved the time-dependent equation (2). The results are presented in Fig. 3.

The behavior of the drag in the stationary regime confirms what is expected from the results of the previous sections. In particular, the critical velocity for the onset of dissipation is lower than c_∞. The reason for this is that, in the region of the

repulsive obstacle, the density decreases and conservation of flux requires that the local fluid velocity increases. As a result, it may happen that Landau's criterion is verified (although $v_\infty<c_\infty$) because the *local* fluid velocity reaches the sound velocity. For slowly varying potentials (i.e., in the regime $\sigma\gg\xi$) this argument was put on a firm mathematical basis by Hakim [22].

From this, one can infer that for *attractive potentials* instead, the critical velocity should be equal to c_∞ since for such potentials the density increases in the region of the obstacle and the local velocity decreases accordingly [23]. This has already been observed in the case of a δ-peak potential (see Fig. 1) and also for an attractive square well (see Ref. [15]). We have performed numerical checks showing that the same occurs for an attractive Gaussian potential. We will return in the final section to the difference between attractive and repulsive potentials.

Let us now come to the discussion of the time-dependent data (the circles of Fig. 3). They are drawn with error bars: this does not correspond to a numerical uncertainty, but reflects the fact that the drag depends on time in the nonstationary regime. The "error bars" correspond to the extremal values of the time-dependent function $F_d(t)$ (see Fig. 4). The initial condition $\psi(x,t=0)$ was taken as the stationary superfluid solution in the presence of the potential for the subsonic case $v_\infty^{\text{init}}=0.5c_\infty$, to which a Galilean boost $\exp\{i(v_\infty^{\text{init}}-v_\infty)x\}$ was applied at $t=0$ in order to reach the desired value of velocity. Accordingly, in the computation, the drag $F_d(t)$ starts from 0 and after a setup time reaches a regime where it oscillates around a mean value (see Fig. 4), which is represented by the circles in Fig. 3. The oscillations of $F_d(t)$ around its mean value are of interest because they reflect the cause of time dependence of the flow: the numerics indicate
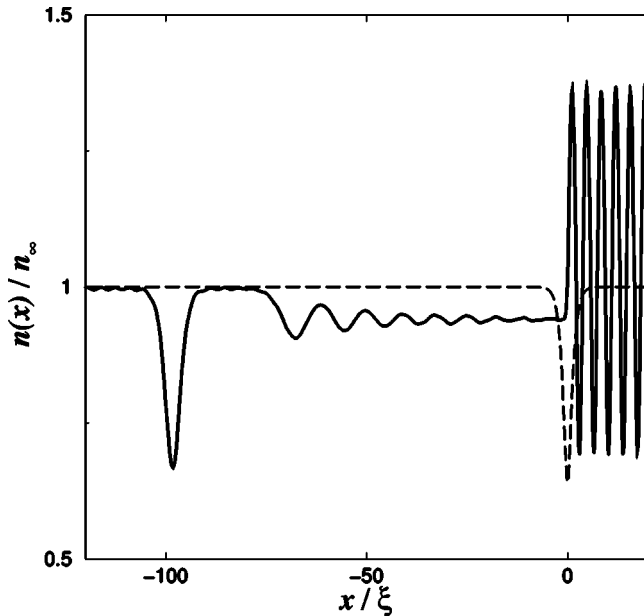
FIG. 5. Density profile in the case $v_\infty = 1.6 c_\infty$, in the presence of a Gaussian potential ($V_0 \xi^2 = 0.2$, $\sigma = 0.5\xi$). The plot represents the profile (solid line) after evolution of the initial $n(x, t = 0)$ (dashed line) during a time t with $v_\infty t / \xi = 203.6$. The density trough initially located at $x = 0$ has moved to the left and is now at $x \simeq -100\xi$. It will asymptotically move to left infinity. It is followed by a density slightly depressed compared to the initial value n_∞. This depressed density is the asymptotic down-stream density.

that whereas the upstream flow reaches a quasistationary pattern, the downstream density is perturbed by solitons, periodically emitted from the obstacle, that propagate in the same direction as the flow with a smaller velocity (such a behavior has already been observed by Hakim [22]). As illustrated in Fig. 4, the drag decreases when a soliton has just been emitted (this was already noted in two-dimensional flows by Winiecki *et al.* [24], where vortex pairs are emitted from a moving obstacle).

In the supersonic regime, it is also important to discuss the discrepancy between the results for the drag computed for stationary flows and for time dependent ones (solid line and circles, respectively, in Fig. 3). This discrepancy by no means implies that the stationary profile is unstable or that the asymptotic time-dependent flow is not stationary. On the contrary, numerics indicate that time-dependent flows reach an asymptotic stationary regime for velocities at which such a regime exists. Moreover, the asymptotic density profile is of the expected type (flat downstream and oscillating upstream). The point is that our specific initial condition $\psi(x, 0)$ does not asymptotically lead (when $t \to \infty$) exactly to downstream density and velocity which have the same value n_∞ and v_∞ as the initial flow. This is illustrated in Fig. 5. In the figure, one sees that the asymptotic downstream density is about 6% lower than n_∞ and a simple numerical check shows as well that the asymptotic velocity differs from v_∞ (is roughly 3% higher). This artifact becomes less and less important for increasing velocities: since the perturbative approach is more and more accurate, it is clear that downstream modifications of the solution become minor and that the

asymptotic solution is the expected one. As a result, when v_∞ increases, the black circles get closer to the solid line in Fig. 3.

IV. DISCUSSION AND CONCLUSION

The above-presented results illustrate the well-known fact that nonlinear effects alter the simple perturbative (Landau's) approach for the determination of the critical velocity at which dissipation occurs (we saw, however, that the perturbative approach could reach a regime of accuracy at large velocity). For repulsive potentials, the critical beam velocity is smaller than the velocity of sound c_∞ (which is here the critical velocity from Landau's criterion) because, in the region of the potential, the local fluid velocity can reach values higher than the sound velocity. The onset of dissipation corresponds to nonstationary flows with a wake asymptotically extending upstream to infinity, and downstream periodic emission of solitons. In fact, another way of explaining the lower stability of the dissipationless flow in the presence of a repulsive potential is to remark that, for subsonic flow over such an obstacle, the density decreases in the region of the potential, allowing easier nucleation of solitons.

On the other hand, we have shown that, for attractive potentials, stationary dissipationless solutions exist up to $v_\infty = c_\infty$: Bose-Einstein condensates appear to be excellent supports for reaching Landau critical velocity, more appropriate than superfluid helium, because, in atomic vapors, it is simpler to contruct obstacles described by purely attractive potentials.

We also showed, using analytical and numerical examples, that stationary dissipative profiles exist in hypersonic beams, provided the beam velocity is large enough. From the numerical study, these solutions seem stable, and moreover time-dependent flows tend asymptotically to such solutions (when they exist). It is interesting to note that dissipation is drastically reduced at very high velocity, i.e., superfluidity is recovered. Such an effect should also exist in higher dimensions for penetrable potentials. It can be understood perturbatively: at high velocity, when the perturbative approach becomes valid, the relevant wave vector (denoted κ in Sec. III A) is large and the Bogoliubov dispersion relation becomes exactly quadratic. Hence, in this regime one has a matter wave described by the linear Schrödinger equation. The drag in this regime can be shown to be proportional to the reflection coefficient, which, as is well known, decreases at high energy (in any dimension).

Note that, for the sake of clarity, we have always illustrated our conclusions using rather weak perturbing potentials. The reasons for this are twofold: (i) for stronger potentials the supersonic stationary regime that we wanted to emphasize is rejected to higher velocity; (ii) the numerical effort necessary in the study of the nonstationary regime is decreased for weak potentials since the domain of time dependence is reduced.

Although for stronger potentials the qualitative results remain the same, very interesting new quantitative phenomena occur. In particular, enormous differences in drag can occur when switching from repulsive to attractive potentials (pro-
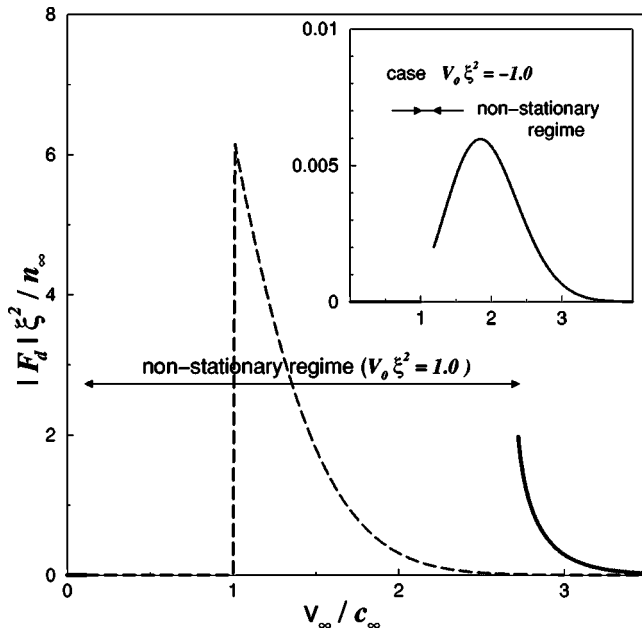
FIG. 6. Drag exerted by a low-density beam on a Gaussian potential ($V_0 \xi^2 = \pm 1.0$, $\sigma/\xi = 1.0$), as a function of the beam velocity. The conventions are the same as in Fig. 2. The main figure displays the drag for a repulsive potential (solid line) together with the perturbative result (13) (dashed line) which is not affected by the sign of the potential. The inset displays an enlargement of the main figure allowing to see the (very small) drag for an attractive potential.

vided the potential is strong enough). This is illustrated in Fig. 6.

One sees in the figure that the domain of existence of stationary solutions is markedly different between attractive and repulsive potentials and that the values of the drag differ by more than two orders of magnitude. The physical explanation for this phenomenon is subtle. At high velocity, contrarily to intuition, the density decreases (increases) in an attractive (repulsive) potential [25]. Hence, an attractive potential creates a density trough which, being the supersonic analog of a gray soliton, does not create large perturbations

in its wake. This results in a small drag. This feature is clearly missed by the perturbative approach, which gives a drag insensitive to the sign of the potential [see Eq. (13)].

From the result of Fig. 6 it would be very interesting to redo with an *attractive* perturbing potential the experiments which have been done at MIT with a repulsive potential [12,13]. Although the present computations are valid in a quasi-one-dimensional regime (whereas the experiments were done in truly three-dimensional systems), the present results leave no doubt that the critical velocity for the onset of dissipation should increase and that the energy transfer rate from the obstacle to the fluid (i.e., $F_d v_\infty$) should drastically decrease in the case of an attractive obstacle [26].

Finally, we note that the present discussion sheds some light on the theory of wave resistance. The wave resistance is the part of the drag experienced by a body moving in a medium which is caused by excitation of waves in this medium (typically surface waves in the case of boats). In a superfluid, a $T=0$ (i.e., in the present work), this is the only source of drag (if one broadens its definition in order to include nonlinear effects such as vortex or soliton formation). Recent experiments of moving spheres in silicone oil [27] have shown that the wave resistance at Landau threshold has a smooth behavior as a function of the velocity, contrary to the expectation of perturbation theory [28]. The same behavior was found here: nonlinear effects smoothe out the unphysical step in drag predicted by perturbation theory. This smooth behavior was already observed in the experiments done at MIT [12,13] and in numerical simulations by Frisch *et al.* [29] and Winiecki *et al.* [24] when moving an impenetrable sphere in a superfluid. Hence, Bose-condensed systems offer an interesting testing ground for ubiquitous nonlinear hydrodynamical effects, in a particularly simple theoretical framework (the Gross-Pitaevskii equation).

ACKNOWLEDGMENTS

[1] M.J. Renn *et al.*, Phys. Rev. A **55**, 3684 (1997); D. Müller, E.A. Cornell, D.Z. Anderson, and E.R.I. Abraham, *ibid.* **61**, 033411 (2000).

[2] J. Denschlag, D. Cassettari, and J. Schmiedmayer, Phys. Rev. Lett. **82**, 2014 (1999); M. Key *et al.*, *ibid.* **84**, 1371 (2000); J.A. Richmond *et al.*, Phys. Rev. A **65**, 033422 (2002).

[3] N.H. Dekker *et al.*, Phys. Rev. Lett. **84**, 1124 (2000); W. Hänsel, J. Reichel, P. Hommelhoff, and T.W. Hänsch, *ibid.* **86**, 608 (2001).

[4] K. Bongs *et al.*, Phys. Rev. A **63**, 031602 (2001).

[5] W. Hänsel, P. Hommelhoff, T.W. Hänsch, and J. Reichel, Nature (London) **413**, 498 (2001).

[6] H. Ott *et al.*, Phys. Rev. Lett. **87**, 230401 (2001).

[7] A.E. Leanhardt *et al.*, e-print cond-mat/0203214.

[8] P. Cren *et al.* Eur. Phys. J. D e-print cond-mat/0203618.

[9] L.D. Landau, J. Phys. (Moscow) **5**, 71 (1941), reprinted in I.M. Khalatnikov, *An Introduction to the Theory of Superfluidity* (Perseus Publishing, Cambridge, 2000).

[10] R. P. Feynman, in *Progress in Low Temperature Physics*, edited by C. J. Gorter (North-Holland, Amsterdam, 1957), Vol. I, p. 17.

[11] However, in liquid helium II, Landau's limit can be reached in some specific cases, see, e.g., P. V. E. McClintock and R. M. Bowley, *Progress in Low Temperature Physics*, edited by W. P. Halperin (Elsevier, Amsterdam, 1995), Vol. XIV, p. 2.

[12] C. Raman *et al.*, Phys. Rev. Lett. **83**, 2502 (1999).

[13] R. Onofrio *et al.*, Phys. Rev. Lett. **85**, 2228 (2000).

[14] S. Inouye *et al.*, Phys. Rev. Lett. **87**, 080402 (2001).

[15] P. Leboeuf and N. Pavloff, Phys. Rev. A **64**, 033602 (2001).

[16] A.D. Jackson, G.M. Kavoulakis, and C.J. Pethick, Phys. Rev. A **58**, 2417 (1998).

[17] Note that we consider a quasi-1D system with infinite coherence length, and discard from the present study quasicondensates such as observed by S. Dettmer *et al.*, Phys. Rev. Lett. **87**, 160406 (2001). In fact, we can also describe quasicondensates. The assumption made is that the temperature is low enough so that the coherence length is large compared to the size of the structure we describe (typically a few times the relaxation length).

[18] T is constructed from the Lagrangian density $\mathcal{L}[\psi,\psi^*,x]$, from which Eq. (2) is derived: $T = -\partial_x\psi\partial\mathcal{L}/\partial[\partial_x\psi] - \partial_x\psi^*\partial\mathcal{L}/\partial[\partial_x\psi^*]+\mathcal{L}$; see, e.g., G. Wentzel, *Quantum Theory of Fields* (Interscience, New York, 1949).

[19] F. Dalfovo, S. Giorgini, L.P. Pitaevskii, and S. Stringari, Rev. Mod. Phys. **71**, 463 (1999).

[20] Even in the subsonic regime, one finds stationary solutions with a wake corresponding to dissipation. However, these solutions are presumably unstable, whereas the solutions localized on the perturbation are found to be numerically stable. Besides, when varying v_∞/c_∞ and the strength of the potential, one finds that the dissipative subsonic solutions have a smaller domain of existence than the superfluid ones: i.e., on the edge of the domain of superfluidity, the localized dissipationless solutions are the only existing ones (see Ref. [15]).

[21] Superfluid behavior at supersonic speed has already been found for other specific potentials: C.K. Law, C.M. Chan, P.T. Leung, and M.-C. Chu, Phys. Rev. Lett. **85**, 1598 (2000).

[22] V. Hakim, Phys. Rev. E **55**, 2835 (1997).

[23] Taking into account modifications of the Bogoliubov spectrum which go beyond our adiabatic ansatz (1) slightly alters this oversimplified view and leads to a critical velocity slightly smaller than c_∞, even for attractive potentials; see P.O. Fedichev and G.V. Shlyapnikov, Phys. Rev. A **63**, 045601 (2001).

[24] T. Winiecki, J.F. McCann, and C.S. Adams, Phys. Rev. Lett. **82**, 5186 (1999).

[25] This is most clearly seen in the perturbative regime $\kappa\sigma \gg 1$ and $V_0 \ll \kappa^2$, where Eq. (10) leads to $\delta A(x) = 2\,\mathrm{sgn}(v_\infty - c_\infty)\kappa^{-2}\sqrt{n_\infty}V_\parallel(x)$.

[26] Moreover, the experiments can been done in the same quasi-1D regime as the present theory, by taking as an obstacle a laser whose waist is much larger than the transverse size of the condensate.

[27] T. Burghelea and V. Steinberg, Phys. Rev. Lett. **86**, 2557 (2001).

[28] E. Raphaël and P.-G. de Gennes, Phys. Rev. E **53**, 3448 (1996).

[29] T. Frisch, Y. Pomeau, and S. Rica, Phys. Rev. Lett. **69**, 1644 (1992).